J-Researchers

JOURNAL OF CIVIL ENGINEERING RESEARCHERS

Modeling and characterization of fiber-reinforced (FRP) plastic honeycomb sandwich panels for bridge deck

Ali nazemideylami [a,*]

[a] *Ms.c, Department of Civil Engineering, Takestan Branch, Islamic Azad University, Qazvin, Iran*

Journals-Researchers use only: Received date: 2023.06.01; revised date: 2023.07.11; accepted date: 2023.07.22

Abstract

Several factors and reasons, including correcting errors in bridge design and construction, preventing damage caused by natural and environmental factors, forces caused by earthquakes, or strengthening the bridge structure to withstand more loads, increase the need to strengthen the bridge. Reinforcement is usually applied to a specific element in the bridge, such as the foundation, column, beam head and deck, each of which may be reinforced. Also, from the economic point of view, retrofitting of bridges is generally preferred compared to the replacement and renovation option. Bridges play an important role in rescue operations after an earthquake. It is necessary that these structures have a higher level of protection against seismic attacks. The earthquake identified the weak points of the structure. Bridges are very vulnerable to these attacks due to their low degree of uncertainty. Seismic displacements based on the principles of elastic design are much less than what the structure experiences in a real earthquake. One of the consequences is the falling of the decks due to the loss of the support surface. The decision to strengthen the bridge was made when many bending and shear cracks were created on the king beams of the bridge. The use of FRP profiles can significantly prevent losses caused by corrosion and is a good alternative to traditional methods of strengthening the structure. In this article, the design for the deck of a sandwich panel bridge reinforced with FRP fibers is presented. (DOI:**https//doi.org/10.52547/JCER.5.3.51**)

*Keywords:*FRP; Glass fibers; Bridge decks; Pultrusion; Materials tests; Optimization

1. Introduction

At present, two major types of FRP deck are currently used in engineering works; Sandwich structure and pultruded structure. Sandwich structures consist of strong, high-stiffness top sheets that can withstand bending loads and have very low density. The core of shear strength is placed between the top sheet and the bottom sheet, which determine the performance of the deck composite. The top sheets are usually made of matrial E-glass or a top of polyester or vinyl ester. The core materials are rigid foam or FRP materials in the form of thin-walled cells shown in Figure 1. Cellular materials are the most important

* Corresponding author. Tel.: +98-911-243-5320; e-mail: Nazemideylami@gmail.com.

materials for structural weight-sensitive applications. Figure 2 shows the sections of the FRP bridge deck.

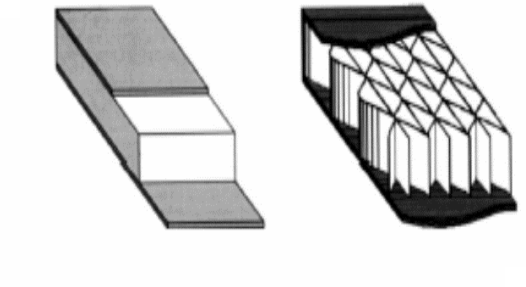

Fig. 1. Examples of types of bridge structures with FRP decks [1]

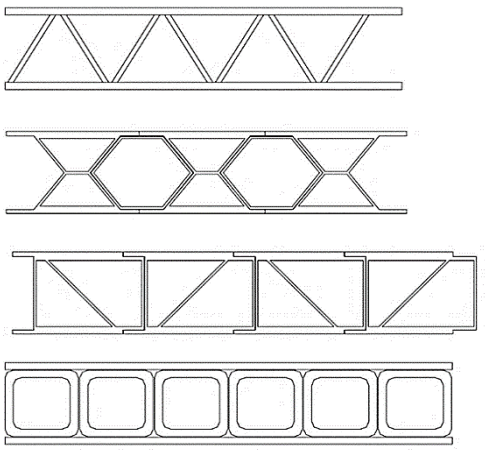

Fig. 2. Types of FRP bridge deck sections. [1]

The failure mechanism in different panels is different according to their load transfer type. For example, the transfer of load in a triangular panel is two-way, and in honeycomb panels, the load is transferred to the four sides of the transfer edge and then transferred to the support. In the following, in this report, the types of panel ruptures (abrasion rupture, shear rupture, bending strain, etc.) are explained and how the load is transferred in all types of panels according to the inner core. An example of failure is presented in Figure 3 related to the triangular panel.

The ability to transfer the load of the honeycomb core of the panel is not completely clear. Therefore, to determine the effective width of the design, it is necessary to consider some assumptions. For this investigation, assumptions based on AASHTO (1996) standard specifications for concrete slabs were considered. AASHTO distinguishes between two types of slabs supported at two edges: reinforced perpendicular to the axis of traffic and reinforced parallel to the axis of traffic. The optimization of the deck has been done without considering the required properties of the deck, such as the performance of the composite and the design between the deck and its supports. Advantages such as increasing the hardness and resistance of the system as well as the economic design of the bridge regarding the performance and layout of the composite should be considered. In this case, the bending behavior of the deck in the plane will be very effective, and this motivation and interest made the performance advantages of the composite core in the bridge deck to be selected for study. An example of the geometry of triangular FRP bridge deck panels is shown in Figure 4.

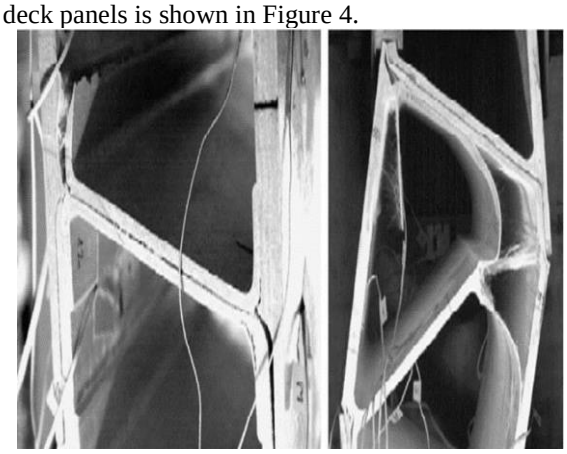

Fig. 3. Break in the triangular panel [1]

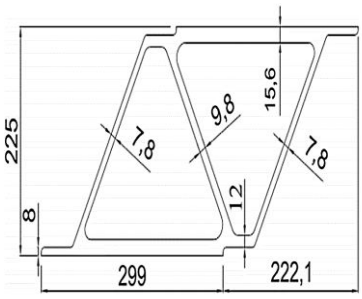

Fig. 4. An example of a triangular cross section geometry in an FRP deck [1]

The shear failure of FRP sandwich panels is completely different from the shear failure observed

for reinforced concrete structures. According to the published documents, the shear rupture of the panels usually begins with the tearing and separation of the upper surface from the core. Therefore, an FRP panel fails in shear when the shear stress between the top and core interface reaches the contact shear strength. Figure 5.

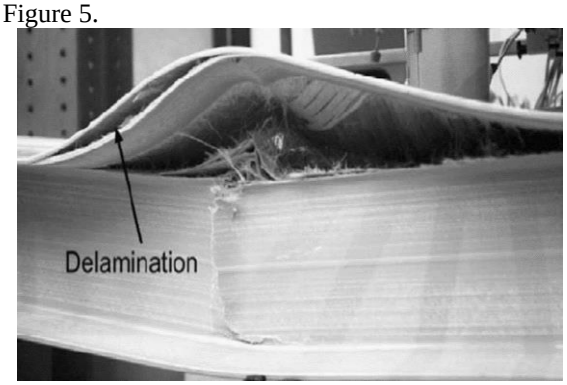

Fig. 5. Shear failure in FRP bridge deck [1]

2. Slab production process

Honeycomb core panels are generally constructed for one-way bending around the x2 axis as shown in. For this reason, most of the past research has focused on the tensile strength of materials around the x1 axis. This study focuses on the load-carrying behavior of glass fiber reinforced polymer (GFRP) bridge deck panels manufactured by Kansas Structural Composites, Inc. (KSCI) using a hand lay-up technique. The deck panels are constructed using a sandwich panel configuration, which consists of two stiff faces separated by a lightweight core. The core has a sinusoidal wave configuration in the x1-x2 plane, as shown in Figure 6.

The sinusoidal wave has an amplitude of 2 in. and the core material has a thickness of 0.09 in., as shown in Figure 6-1(b). Figure 6-1(b) shows a Representative Volume Element (RVE), which is a single basic cell that is repeated periodically to form the core structure. The panel was designed for one-way bending about the x2 axis. Therefore, the bending stiffness about the x2 axis is much higher than that about x1. Plunkett (1997) described in detail the panel manufacturing process. The honeycomb core is composed of a flat GFRP sheet bonded to a corrugated GFRP sheet as shown in Figure 2-1. The core flat parts are laid up on a flat surface with vinylester resin manually applied to chopped strand mat reinforcement. The corrugated parts are fabricated in the same fashion as the flat parts but on corrugated molds. The flat parts are then placed on top of the wet corrugated parts to produce a bond as the corrugated parts cure. The face is composed of fiberglass fabric layers, which are wet in resin and laid up upon each other until desired face thickness is obtained. To increase the interface shear strength between the core and the faces, a new detail is introduced in the manufacturing process for the O'Fallon Park bridge panels. In the panels, GFRP mats are inserted between the core and the faces at about 13 in. distance as shown in Figure 7(b)

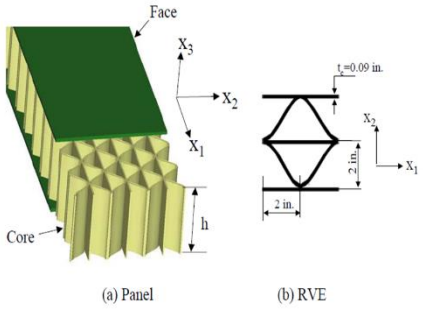

Fig. 6. Configuration of the core and the faces [1]

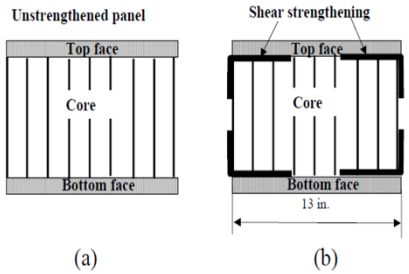

Fig. 7. Shear strengthening details

3. Design Requirements

For this bridge, the design live load specified is an HS 25 truck. This leads to a design wheel load of 20 kips. With an impact factor of 30%, the design load becomes 26 kips per wheel. Tire Contact Area in the AASHTO LFRD Specifications (1998), the tire

contact area is considered a rectangle with a width of 20 in. and a length l given by:

$$l = 2.28\gamma\left(1 + \frac{IM}{100}\right)P \quad (1)$$

Where γ is the load factor, IM is the impact factor, and P is the wheel load. For this case, γ = 1.75, IM = 30, and P=20 kips. Hence, l=19 in. which leads to a contact area of 380 square inches.

The load transfer capability of a honeycomb panel is not well understood. Therefore, to determine the effective width for design, some assumptions are necessary. For this evaluation, assumptions were made based on the AASHTO Standard Specifications (1996) for concrete slabs. AASHTO distinguishes

between two cases for slabs supported along two edges: (1) main reinforcement perpendicular to the traffic, and (2) main reinforcement parallel to the traffic. In the first case, the live load moment for a simple span shall be determined by the following formula (impact not included):

$$M = \left(\frac{S+2}{32}\right)P \; Moment\; on\; foot - pounds\; per\; foot - width\; of\; slab \quad (2)$$

Where S is the effective span length in feet and P is the wheel load in pounds. For slabs continuous over more than two supports, the effective span is defined as the clear span. To estimate the effective bending width for a one-way slab, the load per foot-width of a slab is given as:

$$P = \frac{4M}{S}\; load\; in\; pounds\; per\; foot - width\; of\; slab \quad (3)$$

The effective bending width in feet is then calculated as follows:

$$W_b = \frac{P}{\bar{P}} \quad (4)$$

Deflection Criterion According to the City and County of Denver provisions, the panel should be designed so that the deflection due to service load plus impact shall not exceed 1/1000 of the span length. Flexure Criteria Section 600 of the City and County of Denver provisions suggests using both Allowable Stress Design and Load Factor Design approaches as follows. The maximum strain shall be limited to 20% of the ultimate strain under service loads and the maximum dead load strain shall be limited to 10% of the ultimate strain.

The maximum Factored Load shall be given by:

$$P = 1.3x(1.67x(LLxIM) + DL) \quad (5)$$

and it shall not exceed 50% of ultimate load capacity. In equation (4.5), LL is the Live Load, IM is the Impact Factor, and DL is the Live Load.

Shear Criteria The shear failure mode for the honeycomb sandwich panel used for the O'Fallon bridge deck is expected to be different from that for reinforced concrete (RC) decks. GFRP sandwich deck fails in shear when a face delaminates from the core, and previous experimental studies (Stone et al. 2001 and Lopez 2001) have shown that this mode is most often the governing failure mode for this type of panel. The shear failure mode for the honeycomb sandwich panel used for the O'Fallon bridge deck is expected to be different from that for reinforced concrete (RC) decks. GFRP sandwich deck fails in shear when a face delaminates from the core, and previous experimental studies (Stone et al. 2001 and Lopez 2001) have shown that this mode is most often the governing failure mode for this type of panel. Section 600 of the City and County of Denver provisions indicates that the maximum Factored Load shall be given by equation (4-5) and it shall not exceed 45% of the ultimate shear load capacity of the deck.

Crushing Criteria, the crushing failure load can be calculated by assuming a contact area of 380 in.2 (AASHTO 1998). According to the provisions of the City and County of Denver (2002), the maximum Factored Load shall be given by equation and it shall not exceed 45% of the crushing failure load.

Thermal Expansion Section 600 of the City and County of Denver provisions states that the supplier has to demonstrate through analysis or testing that the FRP bridge deck structure is thermally compatible with both steel and concrete girder systems.

4. Experiment-Based Modeling

The first verification has used Guido Camata experimental model [3], which tested the honeycomb-shaped slab with a sinusoidal cross-section, and we have used the following method:

1- Modeling the modeled sample of TEST2 under cover analysis by changing the location in the middle of the opening with Abaqus software.

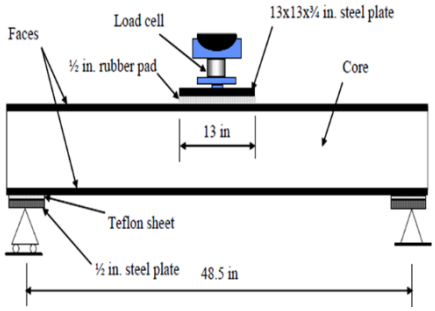

Fig. 8. Geometrical characteristics of the loaded beam [3]

Table. 1.
Geometrical characteristics of the tested beam [3]

	b *in*	h *in*	s *in*	H *in*	H *in*	I in^4
Test1	13	6.5	0.375	7.25	7.43	155
Test2	12	6.5	0.375	7.25	7.43	143
Test3	13	6.5	0.5	7.5	7.68	201
Test4	13	6.5	0.5	7.5	7.68	201

2- Comparing the outputs obtained from the TEST2 model from the Abaqus software with the results obtained from the laboratory.

In short, we can say that after introducing the materials to the Abaqus software, the modeled sample TEST2 has been subjected to wear analysis by applying displacement in the middle of the opening, the results of which are given in the following discussion. As shown in Figure 8, according to the experiments conducted by Guido Camata who tested the honeycomb slab with sinusoidal cross-section, the geometric characteristics of this beam are given in Table 1.

We used the research of Mr. Davalos [4] to introduce the materials. In this article, micromechanics theories are presented for calculating isotropic materials for modeling composite slabs, both as a real geometric cross-section of the slab and very simplified for manual calculations using an equivalent cross-section. The characteristics of its isotropic materials are presented according to table (2).

Figure 9 shows how force is applied to the beam in the laboratory. Figure 10 shows the separation of the upper part from the core of the beam under load in the laboratory. After the separation of the upper part from the core of the beam under load, it showed its resistance in the form of buckling of the slab components. What is clear is that the shear reinforcement is for the beam at this time, and it has caused a better cohesion of the slab and prevented its immediate separation and caused it to behave more malleable.

Fig.9 .How to apply force in the laboratory [3]

Fig.10. Separation of the upper surface from the core of the beam under load in the laboratory [3]

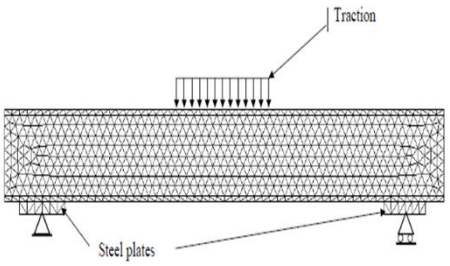

Fig.11. Schematic loading on beam [3]

As mentioned above, shear reinforcement is used to prevent the instantaneous buckling of the slab after the separation of the top from the core, but before the separation, it increases the bending strength due to the increase in the thickness of the top.

Table 2
Layer stiffness properties obtained from micromechanics model

Ply name	Orientation	E_1(Gpa)	E_2(Gpa)	G_{12}(Gpa)	G_{23}(Gpa)	v_{12}	v_{23}
Bond layer	Random	*9.72*	*9.72*	*3.5*	*2.12*	*0.394*	*0.401*
CM3205	0^0or 90^0	*27.72*	*8.00*	*3.08*	*2.88*		*0.390*
	Random	*11.79*	*11.79*	*4.21*	*2.36*	*0.295*	*0.400*
						0.402	
UM1810	0^0	*30.06*	*8.55*	*3.30*	*3.08*		*0.386*
	Random	*15.93*	*15.93*	*5.65*	*2.96*	*0.293*	*0.388*
						0.409	
Core mat	Random	*11.79*	*11.79*	*4.21*	*2.97*	*0.402*	*0.388*

stiffness properties laminates

	E_X,GPa(*10^6 psi)	E_Y,GPa(*10^6 psi)	V_{xy}	G_{xy},GPa(*10^6 psi)
Face laminate	*19.62(2.846)*	*12.76(1.850)*	*0.302*	*3.76(0.546)*

Figures 11 and 12 show the schematic loading on the beam and its details. This figure indicates that the applied load has occurred in the middle of the beam.

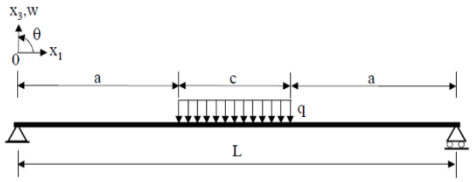

Fig. 12. Schematic loading details on beam

Figure 13 shows the force diagram in terms of displacement of the laboratory sample. This graph indicates that at a force of 80 kips, the displacement will be 0.6.

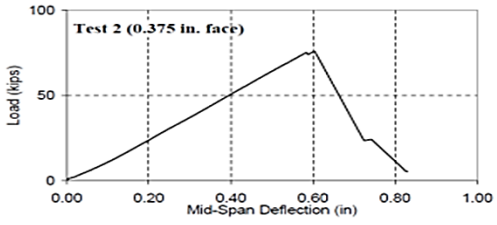

Fig.13. Force diagram according to the change of location of the laboratory sample [3]

5. Modeling with Abaqus finite element software

After introducing the materials to the Abaqus software, the modeled sample TEST2 is subjected to bearing analysis by applying a displacement in the middle of the opening, and during the entire loading period, the resulting force is stored in one of the beam supports, and according to the beam, the applied force in the middle of the opening is equal to twice the reaction value of the support, and in this way, the diagram of the applied force in the middle of the opening according to the displacement according to Figures 16 is drawn, and by comparing it with the laboratory sample, it can be concluded that the behavior of the finite element model is completely similar. According to the laboratory results, it has shown itself. Figure 14 shows the diagram of the force in terms of displacement of the finite element model, which will have a displacement of 0.6 at a load of 70 kips. Figure 15 shows the force diagram in terms of displacement of the laboratory sample, which will have a displacement of 0.6 at a load of 79 kips. Figure 16 is the diagram of the force according to the displacement of the laboratory sample and the software model which shows the comparison of these

two states. These two graphs indicate that the laboratory model has a difference of 1.1%. And the difference is acceptable and the results are very close.

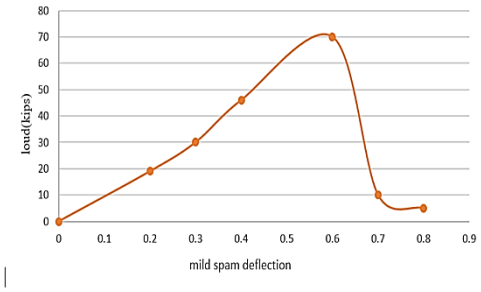

Fig.14. Force diagram according to displacement of the finite element model

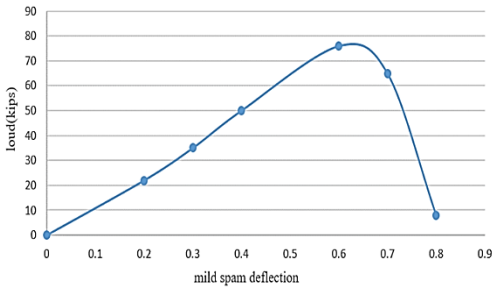

Fig.15. Force diagram according to the change of location of the laboratory sample

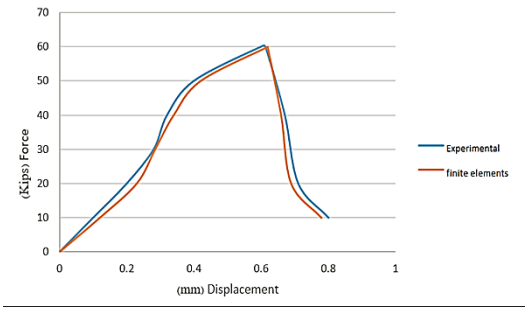

Fig.16. Force diagram according to the change of location of laboratory sample and software model

During loading, after the load reached 70 kips, a slight drop was observed at this point, which indicated the beginning of separation of the top from the core. Finally, the separation spread along the length of the beam and caused the member to break in a brittle manner.

Figure 17 shows the final deformation of the TEST2 finite element model. This figure indicates that there is a concentration of stress on the middle of the opening, which was subjected to a higher load. Also, the stress in the middle of the thickness of the beam indicates that diagonal cracks will occur in the central areas. In the finite element model, the maximum stress is formed in the middle of the opening, which indicates that the maximum bending stress caused the separation of the upper surface from the core, and since the upper surface is under pressure, a brief buckling in any defect will cause the separation of the core from the surface.

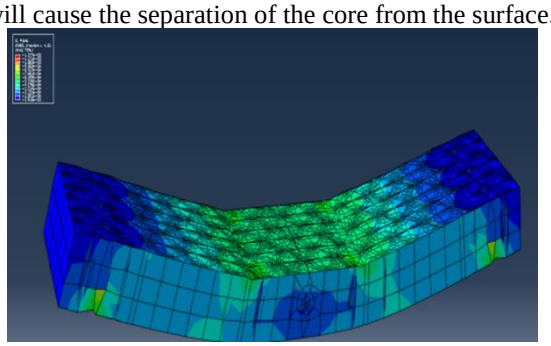

Fig.17. The final transformation of the finite element model TEST2

The abacus model was modified to strengthen against shear, that is, the thickness in the bold parts shown in the figure was 0.09+0.375 inches (Figure 18).

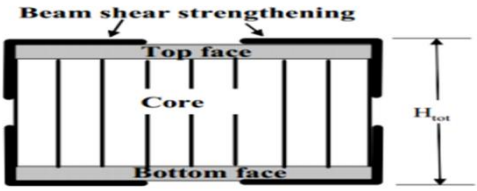

Fig.18. Modified sample

Figure 19 shows the final deformation of the modified TEST2 finite element model. This figure indicates that there is a stress concentration on the pressure area in the middle of the opening, which was subjected to a higher load, and its value will be equal to 1.26 mp. In this part, the ability to create constraints in the area along the support sheet of the software was used. This constraint is introduced to the software in

such a way that the opening length of 48.5 inches is maintained for the finite element model, and also in the area 7.5 inches long from the ends of both sides of the slab, all the element nodes in this area have the same slope according to the reference point that has a vertical support reaction.

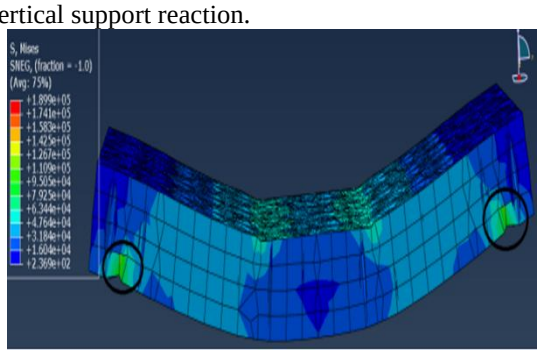

Fig.19. The effect of stress concentration on the local deformation of the modified honeycomb slab at the support

Figure 20 shows the displacement tensor of the beam. This figure indicates that the maximum displacement in the middle of the beam is about 2.2 mm.

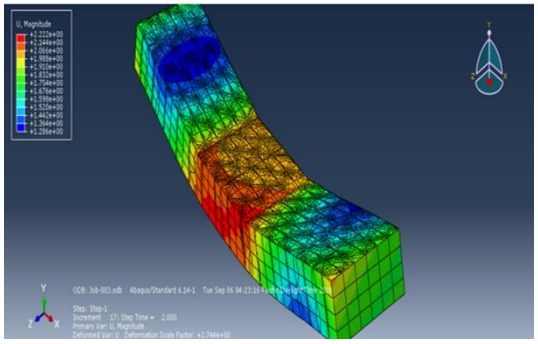

Fig.20. Beam displacement tensor

Figure 21 shows the primary and secondary deformation. And it indicates that the most deformation is related to the middle opening of the beam.

Figure 22 is a diagram showing the shape of the structure. In the case of KIPS70, the maximum displacement is equal to 0.57.

In Figure 23, the shape change diagram of the modeled structure can be seen, which shows the shape change of the structure. In the KIPS70 load, the maximum displacement is equal to 0.5.

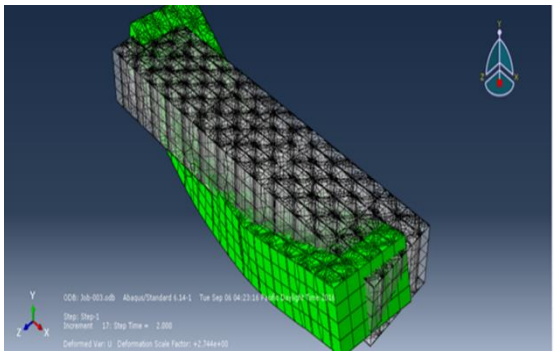

Fig.21. Primary and secondary deformation

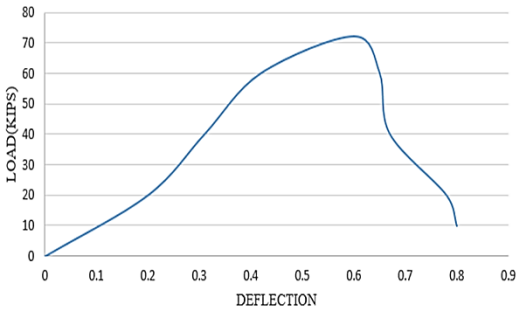

Fig.22. Deformation of the structure in the laboratory

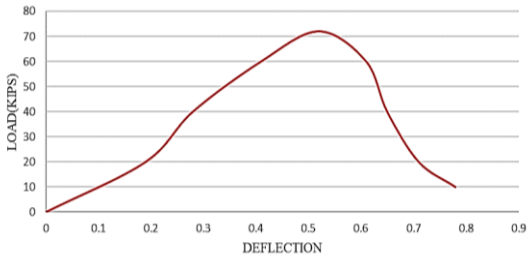

Fig.23. Deformation of the structure in the software in the middle of the opening of the honeycomb slab

Figure 24 shows the comparison diagram of the structural deformation in the software and laboratory model.

Figure 25. The diagram shows stress by distance. This diagram indicates that the maximum stress is on the 25th distance. The intermediate spaces will tolerate the most deformation.

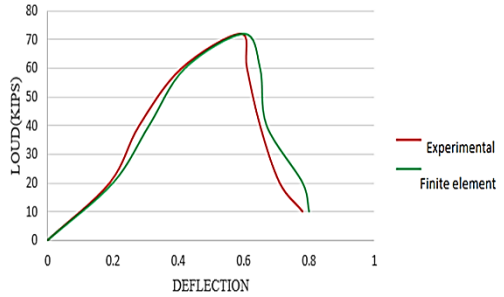

Fig.24. Comparison of structural deformation in the software and laboratory model in the middle of the opening of the honeycomb slab

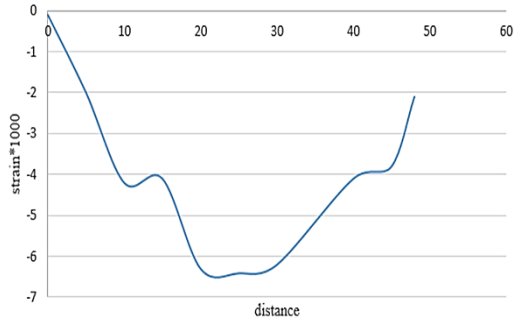

Fig.25. Stress diagram based on distance

6. Conclusion

Comparison of structure deformation in software and laboratory model It indicates that there is not much difference between the obtained results. And the slight difference between the laboratory model and the finite element model is due to the flaws in the laboratory model. According to the initial reports, at the beginning of loading, some of the lamina wires were broken, which had a significant sound. In the finite element model, the maximum stress is formed in the middle of the opening, which indicates that the maximum bending stress caused the separation of the upper surface from the core, and since the upper surface is under pressure, a brief buckling in any defect will cause the separation of the core from the surface. Therefore, this type of member can be investigated and concluded under bending in the finite element model.

Acknowledgments

In the end, I would like to thank my dear teacher Dr. Oskoei and my wife for helping me in this study.

References

[1] Zihong Liu Thomas E. Cousins, Co-Chair, John J. Lesko, Co-Chair, Raymond H. Plaut, Carin L. Roberts Wollmann and Elisa Sotelino. (2007). “Testing and Analysis of a Fiber-Reinforced Polymer (FRP) Bridge Deck”, Doctor of Philosophy in Civil Engineering, Virginia Polytechnic Institute and State University.

[2] Aixi Zhou, John J. Lesko, Co-Chairman, Thomas E. Cousins, Co-chairman, Romesh C. Batra, Scott W. Case and Liviu Librescu. (2002), “STIFFNESS AND STRENGTH OF FIBER REINFORCED POLYMER COMPOSITE BRIDGE DECK SYSTEMS”, Doctor of Philosophy in Engineering Mechanics”, Blacksburg, Virginia, USA

[3] Guido Camata, P. Benson Shing. (2004) “EVALUATION OF GFRP DECK PANEL FOR THE O’FALLON PARK BRIDGE” COLORADO DEPARTMENT OF TRANSPORTATION RESEARCH BRANCH July 2004.

[4] Davalos, J. F., Qiao, P., Xu, F. X., Robinson, J., and Barth, K. E. 2001.“Modeling and characterization of fiber-reinforced plastic honeycomb sandwich panels for highway bridge applications.” Compos. Struct., 523–4, 441–452.

[5] American Association of State Highway and Transportation Officials (AASHTO), “Specifications for Highway Bridges”, Washington, 17th Edition, 2010.

[6] Japan Road Association., (1998)., “Reference For Seismic Retrofit of Existing Highway Bridges”, Maruzeh, Tokyo., Japan.vol. 195. pp.35-45.